This is the peer-reviewed, final accepted version for American Mineralogist, published by the Mineralogical Society of America.
The published version is subject to change. Cite as Authors (Year) Title. American Mineralogist, in press.
DOI: https://doi.org/10.2138/am-2020-7602. http://www.minsocam.org/

LETTER

Effects of small crystallite size on the thermal infrared (vibrational) spectra of minerals

Victoria E. Hamilton*[1], Christopher W. Haberle[2], Thomas G. Mayerhöfer[3,4]

[1]Department of Space Studies, Southwest Research Institute, 1050 Walnut St., #300, Boulder, Colorado 80302, U.S.A (hamilton@boulder.swri.edu)

[2]School of Earth and Space Exploration, Arizona State University, Tempe, Arizona 85287, U.S.A. (chaberle@asu.edu)

[3]Leibniz Institute of Photonic Technology (IPHT), Albert-Einstein-Str. 9, D-07745 Jena, Germany (Thomas.Mayerhoefer@uni-jena.de)

[4]Institute of Physical Chemistry and Abbe Center of Photonics, Friedrich Schiller University, Jena, D-07743, Helmholtzweg 4, Germany

*Corresponding author

This is the peer-reviewed, final accepted version for American Mineralogist, published by the Mineralogical Society of America.
The published version is subject to change. Cite as Authors (Year) Title. American Mineralogist, in press.
DOI: https://doi.org/10.2138/am-2020-7602. http://www.minsocam.org/

Revision 1

ABSTRACT

The thermal infrared (TIR, or vibrational) emission spectra of a suite of synthetic Mg-Fe olivines exhibit notable differences from their natural igneous counterparts in terms of their band shapes, relative depths, and reduced shifts in some band positions with Mg-Fe solid solution. Comparable reflectance spectra acquired from olivine-dominated matrices and fusion crusts of some carbonaceous chondrite meteorites exhibit similar deviations. Here we show that these unusual spectral characteristics are consistent with crystallite sizes much smaller than the resolution limit of infrared light. We hypothesize that these small crystallites denote abbreviated crystal growth and also may be linked to the size of nucleation sites. Other silicates and non-silicates, such as carbonates, exhibit similar spectral behaviors. Because the spectra of mineral separates are used commonly in the modeling and analysis of comparable bulk rock, meteorite, and remote sensing data, understanding these spectral variations is important to correctly identifying the minerals and interpreting the origin and/or secondary processing histories of natural materials.

Keywords: Spectroscopy, olivine, carbonate, crystallinity, metamorphism, meteorites, mineral synthesis, carbonaceous chondrites

INTRODUCTION

Thermal infrared spectroscopy has been used for decades to understand mineral structure and chemistry for applications that range from understanding crystallography to modeling the behavior of minerals under conditions in the Earth's mantle, and even deducing the geologic histories of Solar System objects and the composition of circumstellar disks (Bandfield et

al., 2000; e.g., Burns and Huggins, 1972; Hofmeister et al., 1989; Jäger et al., 1998). For minerals that are not easily obtained through the separation of natural samples, synthesis approaches can be useful for conducting systematic TIR compositional and structural studies (e.g., Maresch and Czank, 1983; Velde, 1980). However, mineral synthesis does not replicate all natural conditions, e.g., starting materials and time. As such, there are opportunities for synthetic minerals to deviate physically, chemically, and thus spectrally from their natural counterparts.

Meteorites, particularly those in the carbonaceous chondrite (CC) class, record some of the earliest geological activity in the Solar System. The CC meteorites are complicated rocks formed by sedimentary processes and they come from parent bodies that did not experience differentiation. They are dominantly comprised of olivines, pyroxenes, phyllosilicates, oxides, sulfides, and carbonates along with Fe,Ni metal. The mineralogy and alteration histories of many meteorites have been explored through TIR spectroscopy, and such spectra have been used to characterize their alteration histories and link them to potentially related asteroids and comets (e.g., Beck et al., 2014; Miyamoto and Zolensky, 1994; Sandford, 1984).

The present study was motivated by several initially unrelated observations. First, we observed that the TIR emission and reflectance spectra of a suite of synthetic olivines (Dyar et al., 2009; Lane et al., 2011) exhibit notable, unexplained, differences in spectral shape and relative band intensity as compared to their igneous counterparts (Hamilton, 2010 and refs. therein). Second, we observed atypical spectral features in microscopic TIR measurements of matrix materials in the CC meteorites Allende (CV_{oxA}) (Hamilton and Connolly Jr., 2012) and Sutter's Mill (C-ungrouped) (Haberle et al., in preparation), as well as aqueously altered CC meteorites that have experienced re-heating (e.g., Hanna et al., 2020; Lee et al., submitted). Third, fusion

crusts on aqueously altered CC meteorites exhibit similarly atypical olivine spectral features. These three sets of spectra represent different origins and histories, but exhibit a remarkable similarity among their spectra that indicates a common physical characteristic, the physics of which have not been described previously to our knowledge.

METHODS

The synthetic and natural olivine emission spectra shown in this work (Figure 1) are taken from Dyar et al. (2009), Lane et al. (2011), Koeppen and Hamilton (2008), and Hamilton (2010); the samples and methods of spectral acquisition are described in detail in those papers.

The carbonaceous chondrite (CC) meteorites analyzed in this work are prepared as polished epoxy mounts (Sutter's Mill) or thin sections (all others) and their thermal infrared reflectance spectra were acquired on a ThermoScientific iN10 Fourier transform infrared microscope (μ-FTIR). The configuration and measurement approach are described by Hamilton (2018) and the spectra can be inverted via Kirchhoff's Law for comparison with spectra acquired in emission (Ruff et al., 1997; Salisbury et al., 1991).

RESULTS

Figure 1 shows spectra acquired from natural (NO) and synthetic (SO) olivine samples spanning the Mg-Fe solid solution series (forsterite, Fo_{100}, to fayalite, Fo_0). Spectral shapes and relative band depths observed in the NO spectra are consistent with other natural samples in the literature (Hamilton, 2010; Koeppen and Hamilton, 2008). Spectra of the SO exhibit nota-

ble differences from the NO, which we describe here in order of decreasing wavenumber (increasing wavelength), using the band nomenclature of Burns and Huggins (1972).

Bands 1-4 are diagnostic silicate (Si-O) stretching vibrations (e.g., Devarajan and Funck, 1975). All four bands are clearly resolved in NO. Band 3 is the most prominent feature, with an asymmetric minimum that is deepest on the high wavenumber side of the band. The positions of these features' minima shift linearly to lower wavenumbers with increasing Fe content (Hamilton, 2010 and references therein). In SO spectra, bands 1 and 2 are weaker, with band 1 commonly appearing as a shoulder. Band 3 is the strongest absorption but differs from NO spectra by having a minimum located centrally or on the low wavenumber side of the feature. Furthermore, the wavenumber range of band 3 as a function of composition (Fo_{90}-Fo_0) is narrower in the SO spectra than in the NO (19 cm^{-1} vs. 30 cm^{-1}). Moreover, the position of band 3 does not consistently decrease with increasing Fe. For example, in the case of SO Fo_{75}, the band 3 position is 879 cm^{-1}, whereas the Fo_{80} and Fo_{70} spectra have minima at 902 and 899 cm^{-1}, respectively (Lane et al., 2011). Similarly, SO Fo_{50} and Fo_{40} samples have band 3 positions that are considerably higher than those determined for Fo_{65} and Fo_{55}. Bands 5-13 span the region from ~667 - 200 cm^{-1} (15 - 50 μm) and arise from the bending and lattice modes of the silicate anion. Here we focus on the relative depths of bands 6 and 7, where band 6 is consistently deeper than band 7 in NO, regardless of position/Fo#. However, in the ~Fo_{70}-Fo_0 SO spectra, band 7 is of equivalent or deeper depth than band 6. The solid solution compositions and purity of the SO were clearly established by Dyar et al. (2009), which suggests that a physical difference between the SO and NO samples is responsible for these spectral trends.

Figure 2a shows μ-FTIR spectra of olivine from an isolated, forsteritic (>Fo_{90}) olivine grain in Allende; the matrix of Allende (~Fo_{50}); a bulk spectrum of the Sutter's Mill meteorite (stone 3); and a fusion crust from the meteorite Elephant Moraine 16100 (EET 16100, CM1). The isolated olivine from Allende (Hamilton and Connolly Jr., 2012) is a large (~200 x 250 μm) polycrystalline grain. It exhibits spectral feature positions and shapes consistent with NO. The olivine-dominated matrix of Allende exhibits spectral feature shapes similar to those described above for SO and is known to be comprised of small (<300 nm - 3 μm), and/or lath-like (1-3 μm x 20 μm) crystals (Watt et al., 2006, and references therein). Sutter's Mill, stone 3, has experienced thermal metamorphism at temperatures >700°C and is dominated by olivine (Haberle and Garvie, 2017; Haberle et al., in preparation). Sharp, asymmetric features in the region of olivine band 3, similar to SO, are attributed to small crystallites of olivine based on XRD data (Haberle et al., in preparation). Similar spectra and XRD patterns have been observed for other naturally and artificially heated carbonaceous chondrites (Hanna et al., 2020; Lee et al., submitted). The spectrum of the fusion crust on EET 16100 also exhibits SO-like weak bands 1 and 2, a sharp, asymmetric band 3, and a deeper band 7 as compared to band 6. Although the dominant mineral in this meteorite is phyllosilicate, frictional heating during atmospheric entry drives off water and quenching results in a composition dominated by olivine, consistent with the meteorite's bulk composition (Blanchard et al., 1974; Fruland, 1974; Genge and Grady, 1999). The olivine grains can be <10 μm (Genge and Grady, 1999).

Discussion

Here we use "fine-" and "coarse-grained" in the petrographic sense and the terms "small crystallites" and "large crystallites" to distinguish the spectral effects of interest to this work. No implications for particle size are intended.

Mayerhöfer (2004 and references therein) has developed a model that enables forward-modeling of IR spectra of materials having different crystallite sizes, where for crystallite sizes, *d*, less than the resolution limit of light (i.e., $d < \lambda/10$, or "small" crystallites), the shape of infrared bands are substantially altered. For larger crystallite sizes, the sample is micro-heterogeneous so that a spectrum taken by a theoretical IR-microscope would depend on the orientation of a single or a few crystallite(s). Macroscopically, a spectrum is then an average of the reflectance of a large number of crystallites. For small crystallites and random orientation, the dielectric tensors is reduced to a scalar and the spectrum recorded with an IR-microscope is the same everywhere on the micro-homogeneous sample as the one recorded macroscopically. Spectral differences due to the different averaging are emphasized where the anisotropy of the single crystal is large. We have applied this model to olivine using the optical constants of Fabian et al. (2001). Figure 2b shows the modeled spectral differences in olivine (~Fo_{95}) having small (average 500 nm) and large (>λ/10) crystallite sizes as compared to SO and NO of similar composition (~Fo_{90}, Figure 1). Where the modeled crystallite sizes are small, the overall spectral contrast between 1100 - 875 cm^{-1} is noticeably reduced, band 1 is reduced in strength relative to bands 2 and 3, and the shape of band 3 becomes strongly distorted, with an inversion and telltale, increasing asymmetry toward the low wavenumber side of the band as observed in SO and fine-grained meteorite olivines. We note that the measured olivine spectra exhibit lesser and/or variable degrees of band position and asymmetry relative to

153 the small crystallite model spectrum; e.g., the band 3 inversion is not observed in the meas-
154 ured spectra, which likely indicates an intermediate or non-uniform range of crystallite sizes in
155 these samples. Band 5 in the small crystallite model spectrum is reduced in strength and the
156 minimum is shifted to lower wavenumbers, also similar to SO and fine-grained meteorite
157 samples. At lower wavenumbers, there is little difference in contrast or spectral shape in any
158 of the four spectra, which we attribute to wavelength-dependent behavior. The modeled
159 spectra do not replicate the relative change in band 6 and 7 depths observed in SO and some
160 meteorite samples but, as noted above, this difference is only observable in compositions
161 <~Fo_{70}. We believe that this model explains the unusual spectral characteristics we have de-
162 scribed for SO and fine-grained meteoritic olivines, an interpretation that also is supported by
163 XRD data as described above.

164 Carbonaceous chondrite meteorites having experienced differing degrees of thermal
165 metamorphism provide a natural sample suite for examining this hypothesis further. Increas-
166 ing thermal metamorphism in CCs is identified by a number of textural and compositional
167 characteristics, but the single most relevant property to our study is the increasing degree of
168 matrix recrystallization (e.g., Huss et al., 2006). Figure 3a presents a series of CC meteorite
169 spectra in order of increasing degree of thermal metamorphism, where the CV3 meteorite is
170 the least metamorphosed and the CK6 is the most metamorphosed. Allende exhibits spectral
171 characteristics that are consistent with small crystallite-dominated matrix olivine. With in-
172 creasing degrees of metamorphism and recrystallization, we observe the progressive devel-
173 opment of spectral features that ultimately are indistinguishable from those of terrestrial nat-
174 ural olivine having the same composition.

This is the peer-reviewed, final accepted version for American Mineralogist, published by the Mineralogical Society of America.
The published version is subject to change. Cite as Authors (Year) Title. American Mineralogist, in press.
DOI: https://doi.org/10.2138/am-2020-7602. http://www.minsocam.org/

175

176 **IMPLICATIONS**

177 The spectral variations that are described here are valuable for interpreting geologic pro-
178 cesses. For example, some of the unusual spectral characteristics attributed here to small crys-
179 tallite sizes in meteoritic olivine are correlated with heating in meteorite matrices (e.g.,
180 Haberle et al., in preparation) or short cooling durations in fusion crust. Such characteristics
181 may therefore also appear in rapidly cooled primary melts. It is possible that additional mod-
182 eling and experimental analysis could lead to a determinative relationship between spectral
183 characteristics and crystallite size or size distribution.

184 Although the focus of this work is olivine, the physics that apply to olivine apply broadly
185 to silicates (e.g., fresnoite, Mayerhöfer (2004)) as well as non-silicates. Figure 3b shows two
186 spectra of the meteorite Grosvenor Mountains 95577 (GRO 95577, CR1) that contain car-
187 bonate absorptions. Some carbonates in this meteorite exhibit similar spectral features to
188 hand samples having large crystallite sizes (e.g., Lane and Christensen, 1997), whereas others
189 exhibit the telltale, low-wavenumber asymmetry that we associate in this work with small
190 crystallite sizes. Although we have not quantitatively determined the crystallite sizes of the
191 carbonates in this meteorite, most carbonate grains in CC meteorites are sufficiently small as
192 to be comprised of small crystallites (e.g., Brearley, 2006; de Leuw et al., 2010) but coarse-
193 grained carbonates can be expected at high degrees of alteration and have been observed in
194 GRO 95577 (Harju et al., 2014). We note that Hardgrove et al. (2016) observed qualitatively
195 similar spectral shape changes in quartz and carbonate that they attributed to surface rough-
196 ness differences on natural sample surfaces; in some cases, it is possible that some of those

shape changes could be due to the presence of small crystallites. Regardless, investigators should be aware of these similarities and a detailed survey of spectral characteristics may be required to distinguish between roughness and crystallite size in unpolished sample spectra. In summary, we've shown here that spectroscopy is a powerful tool for characterizing the crystallite size in common minerals, providing insight into primary and/or secondary formation processes.

Finally, spectral variations that occur as a function of crystallite size could affect the interpretation of natural samples measured in a laboratory (as shown here) or via remote sensing of small body and planetary surfaces. This is particularly relevant for algorithms that rely on fitting the entire spectrum of such materials with an appropriate library of reference spectra (Ramsey and Christensen, 1998; Rogers and Aharonson, 2008). If the crystallite sizes of the minerals in the spectrum to be modeled are not known a priori, examples of each should be included in the spectral library. If only small crystallite spectra are used to model materials comprised of minerals dominated by large crystallites, or vice versa, the best possible result will not be achieved, leading to increased uncertainties in the derived mineralogy.

ACKNOWLEDGEMENTS

A number of colleagues participated in conversations that ultimately led to the understanding presented in this work: Phil Bland, Harold Connolly, Jr. (contributor of the Allende thin section), Laurence Garvie, and Sasha Krot. Don Lindsley generously shared his knowledge about the synthetic samples whose spectra are shown here and he performed an XRD analysis of a different synthetic olivine that was informative but that we ultimately did not incorpo-

rate here. A. D. Rogers and C. Viviano provided valuable reviews that helped clarify several points in this manuscript. U.S. Antarctic meteorite samples are recovered by the Antarctic Search for Meteorites (ANSMET) program which has been funded by NSF and NASA, and characterized and curated by the Department of Mineral Sciences of the Smithsonian Institution and Astromaterials Curation Office at NASA Johnson Space Center.

REFERENCES CITED

Bandfield, J.L., Hamilton, V.E., and Christensen, P.R. (2000) A global view of Martian surface compositions from MGS-TES. Science, 287(5458), 1626-1630.

Beck, P., Garenne, A., Quirico, E., Bonal, L., Montes-Hernandez, G., Moynier, F., and Schmitt, B. (2014) Transmission infrared spectra (2–25 lm) of carbonaceous chondrites (CI, CM, CV–CK, CR, C2 ungrouped): Mineralogy, water, and asteroidal processes. Icarus, 229, 263-277.

Blanchard, M.B., Cunningham, G.G., and Brownlee, D.E. (1974) Comparison of a fusion crust produced by artificial ablation of an olivine with fusion crusts on the Allende and Murchison meteorites. Meteoritics, 9, 316.

Brearley, A.J. (2006) The Action of Water. In D.S. Lauretta, and H.Y. McSween Jr., Eds. Meteorites and the Early Solar System II, p. 587-624. University of Arizona Press, Tucson.

Burns, R.G., and Huggins, F.E. (1972) Cation determinative curves for Mg-Fe-Mn olivines from vibrational spectra. American Mineralogist, 57, 967-985.

de Leuw, S., Rubin, A.E., and Wasson, J.T. (2010) Carbonates in CM chondrites: Complex formational histories and comparison to carbonates in CI chondrites. Meteoritics & Planetary Science, 45(4), 513-530.

Devarajan, V., and Funck, E. (1975) Normal coordinate analysis of the optically active vibrations (k=0) of crystalline magnesium orthosilicate Mg_2SiO_3(forsterite). The Journal of Chemical Physics, 62(9), 3406 - 3411.

Dyar, M.D., Sklute, E.C., Menzies, O.N., Bland, P.A., Lindsley, D., Glotch, T., Lane, M.D., Schaefer, M.W., Wopenka, B., Klima, R., Bishop, J.L., Hiroi, T., Pieters, C., and Sunshine, J. (2009) Spec-

troscopic characteristics of synthetic olivine: An integrated multi-wavelength and multi-technique approach. American Mineralogist, 94(7), 883-898.

Fabian, D., Henning, T., Jäger, C., Mutschke, H., Dorschner, J., and Wehrhan, O. (2001) Steps toward interstellar silicate mineralogy: VI. Dependence of crystalline olivine IR spectra on iron content and particle shape. Astronomy and Astrophysics, 378, 228-238.

Fruland, R.M. (1974) Fusion crust phenomena on some carbonaceous chondrites. Meteoritics, 9, 339.

Genge, M.J., and Grady, M.M. (1999) The fusion crusts of stony meteorites: Implications for the atmospheric reprocessing of extraterrestrial materials. Meteoritics and Planetary Science, 34, 341-356.

Haberle, C.W., and Garvie, L.A. (2017) Extraterrestrial formation of oldhamite and portlandite through thermal metamorphism of calcite in the Sutter's Mill carbonaceous chondrite. American Mineralogist, 102(12), 2415-2421.

Haberle, C.W., Garvie, L.A.J., Christensen, P.R., Hamilton, V.E., Hanna, R.D., Connolly Jr., H.C., and Lauretta, D.S. (in preparation) Evidence for amorphous silicate on the surface of asteroid (101955) Bennu.

Hamilton, V.E. (2010) Thermal infrared (vibrational) spectroscopy of Mg-Fe olivines: A review and applications to determining the composition of planetary surfaces. Chemie der Erde, 70, 7–33.

-. (2018) Spectral classification of ungrouped carbonaceous chondrites I: Data collection and processing. Lunar and Planetary Science, XLIX, Abstract #1759.

Hamilton, V.E., and Connolly Jr., H.C. (2012) In situ microspectroscopy of a Type B CAI in Allende: Mineral identification in petrographic context. Lunar and Planetary Science, XLIII, Abstract #2495, Lunar and Planetary Institute, Houston.

Hanna, R.D., Hamilton, V.E., Haberle, C.W., King, A.J., Abreu, N.M., and Friedrich, J.M. (2020) Distinguishing relative aqueous alteration and heating among CM chondrites with IR spectroscopy. Icarus, 346, 113760.

Hardgrove, C.J., Rogers, A.D., Glotch, T.D., and Arnold, J.A. (2016) Thermal emission spectroscopy of microcrystalline sedimentary phases: Effects of natural surface roughness on spectral feature shape. Journal of Geophysical Research, 121, 542-555.

Harju, E., Rubin, A.E., Ahn, I., Choi, B.-G., Ziegler, K., and Wasson, J.T. (2014) Progressive aqueous alteration of CR carbonaceous chondrites. Geochimica et Cosmochimica Acta, 139, 267-292.

Hofmeister, A.M., Xu, J., Mao, H.-K., Bell, P.M., and Hoering, T.C. (1989) Thermodynamics of Fe-Mg olivines at mantle pressures: Mid- and far-infrared spectroscopy at high pressure. American Mineralogist, 74, 281-306.

Huss, G.R., Rubin, A.E., and Grossman, J.N. (2006) Thermal metamorphism in chondrites. In D.S. Lauretta, and H.Y. McSween, Eds. Meteorites and the Early Solar System II, p. 567-586. The University of Arizona Press, Tucson.

Jäger, C., Molster, F.J., Dorschner, J., Henning, T., Mutschke, H., and Waters, L.B.F.M. (1998) Steps toward interstellar silicate mineralogy: IV. The crystalline revolution. Astronomy and Astrophysics, 339, 904-916.

Koeppen, W.C., and Hamilton, V.E. (2008) Global distribution, composition, and abundance of olivine on the surface of Mars from thermal infrared data. Journal of Geophysical Research, 113(E05001), doi:10.1029/2007JE002984.

Lane, M.D., and Christensen, P.R. (1997) Thermal infrared emission spectroscopy of anhydrous carbonates. Journal of Geophysical Research, 102(E11), 25581-25592.

Lane, M.D., Glotch, T.D., Dyar, M.D., Pieters, C.M., Klima, R., Hiroi, T., Bishop, J.L., and Sunshine, J. (2011) Mid-infrared spectroscopy of synthetic olivines: Thermal emission, specular and diffuse reflectance, and attenuated total reflectance studies of forsterite to fayalite. Journal of Geophysical Research, 116(E08010), doi:10.1029/2010JE003588.

Maresch, W.V., and Czank, M. (1983) Phase characterization of synthetic amphiboles on the join $Mn_x^{2+}Mg_{7-x}[Si_8O_{22}]$ $(OH)_2$. American Mineralogist, 68, 744-753.

Mayerhöfer, T.G. (2004) Modelling IR-spectra of single-phase polycrystalline materials with random orientation — a unified approach. Vibrational Spectroscopy, 35, 67-76.

Miyamoto, M., and Zolensky, M.E. (1994) Infrared diffuse reflectance spectra of carbonaceous chondrites: Amount of hydrous materials. Meteoritics, 29, 849–853.

Ramsey, M.S., and Christensen, P.R. (1998) Mineral abundance determination: Quantitative deconvolution of thermal emission spectra. Journal of Geophysical Research, 103, 577-596.

Rogers, A.D., and Aharonson, O. (2008) Mineralogical composition of sands in Meridiani Planum determined from Mars Exploration Rover data and comparison to orbital measurements. Journal of Geophysical Research, 113(E06S14), E06S14.

309 Ruff, S.W., Christensen, P.R., Barbera, P.W., and Anderson, D.L. (1997) Quantitative thermal
310 emission spectroscopy of minerals: A laboratory technique for measurement and calibra-
311 tion. Journal of Geophysical Research, 102, 14899-14913.
312 Salisbury, J.W., D'Aria, D.M., and Jarosewich, E. (1991) Midinfrared (2.5-13.5 μm) reflectance
313 spectra of powdered stony meteorites. Icarus, 92, 280-297.
314 Sandford, S.A. (1984) Infrared transmission spectra from 2.5 to 25 μm of various meteorite
315 classes. Icarus, 60, 115-126.
316 Velde, B. (1980) Ordering in synthetic aluminous serpentines; Infrared spectra and cell dimen-
317 sions. Physics and Chemistry of Minerals, 6, 209-220.
318 Watt, L.E., Bland, P.A., Prior, D.J., and Russell, S.S. (2006) Fabric analysis of Allende matrix using
319 EBSD. Meteoritics & Planetary Science, 41(7), 989-1001.
320

This is the peer-reviewed, final accepted version for American Mineralogist, published by the Mineralogical Society of America.
The published version is subject to change. Cite as Authors (Year) Title. American Mineralogist, in press.
DOI: https://doi.org/10.2138/am-2020-7602. http://www.minsocam.org/

FIGURE CAPTIONS

FIGURE 1. Emissivity spectra of coarse particulate (>100 µm), natural (a) and synthetic, pressed powder (b) olivines from *Hamilton* [2010] and *Lane et al.* [2011], respectively. Band positions discussed in the text are indicated with vertical lines located relative to fayalite (Fo_0 or Fo_1) in each dataset; see original references for locations and discussion of other features.

FIGURE 2. (a) Spectra of isolated and matrix olivines from the Allende meteorite (CV_{oxA}), stone 3 of the Sutter's Mill (C) meteorite, and fusion crust from the meteorite EET 16100 (CM1). The isolated olivine grain in Allende exhibits a spectrum consistent with terrestrial igneous olivines, whereas the Allende matrix spectrum exhibits a spectrum having features with relative strengths and asymmetry similar to bands 1-3 in synthetic olivine spectra shown in Figure 1. Sutter's Mill, 3 and the fusion crust exhibit even more pronounced asymmetry at ~870 cm^{-1} and reversed relative band depths at 520 and 495 cm^{-1} (bands 6 and 7). (b) Measured spectra of natural and synthetic olivines with compositions ~Fo_{90} as compared to modeled spectra of olivine (~Fo_{95}) having small and large crystallite sizes.

FIGURE 3. (a) Carbonaceous chondrite meteorite spectra in order (top to bottom) of increasing degree of thermal metamorphism (and recrystallization); all four meteorites are volumetrically dominated by olivine. The dotted line highlights the evolution of the shape and symmetry of band 3 with increasing crystallite size. (b) Spectra from GRO 95577 (CR1) exhibiting dominantly the spectral features of carbonates and phyllosilicates. Carbonate band shapes and shifts

343 characteristic of the presence of grains having large or small crystallites are highlighted by

344 vertical lines at the locations of the carbonate v_3 (~1495 cm^{-1}) and v_2 (~880 cm^{-1}) features.

345

This is the peer-reviewed, final accepted version for American Mineralogist, published by the Mineralogical Society of America.
The published version is subject to change. Cite as Authors (Year) Title. American Mineralogist, in press.
DOI: https://doi.org/10.2138/am-2020-7602. http://www.minsocam.org/

Revision 1

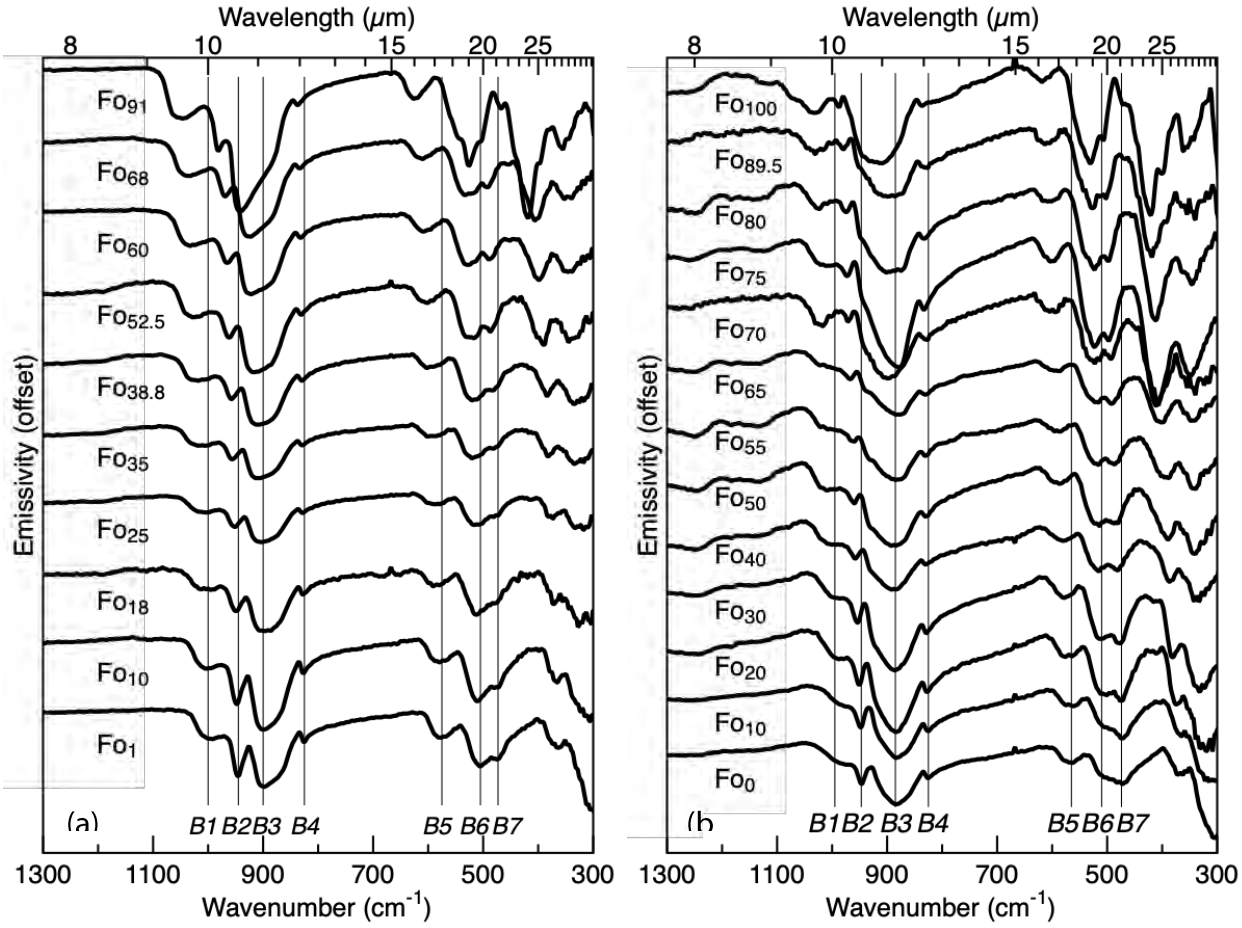

Figure 1.

346

This is the peer-reviewed, final accepted version for American Mineralogist, published by the Mineralogical Society of America.
The published version is subject to change. Cite as Authors (Year) Title. American Mineralogist, in press.
DOI: https://doi.org/10.2138/am-2020-7602. http://www.minsocam.org/

Revision 1

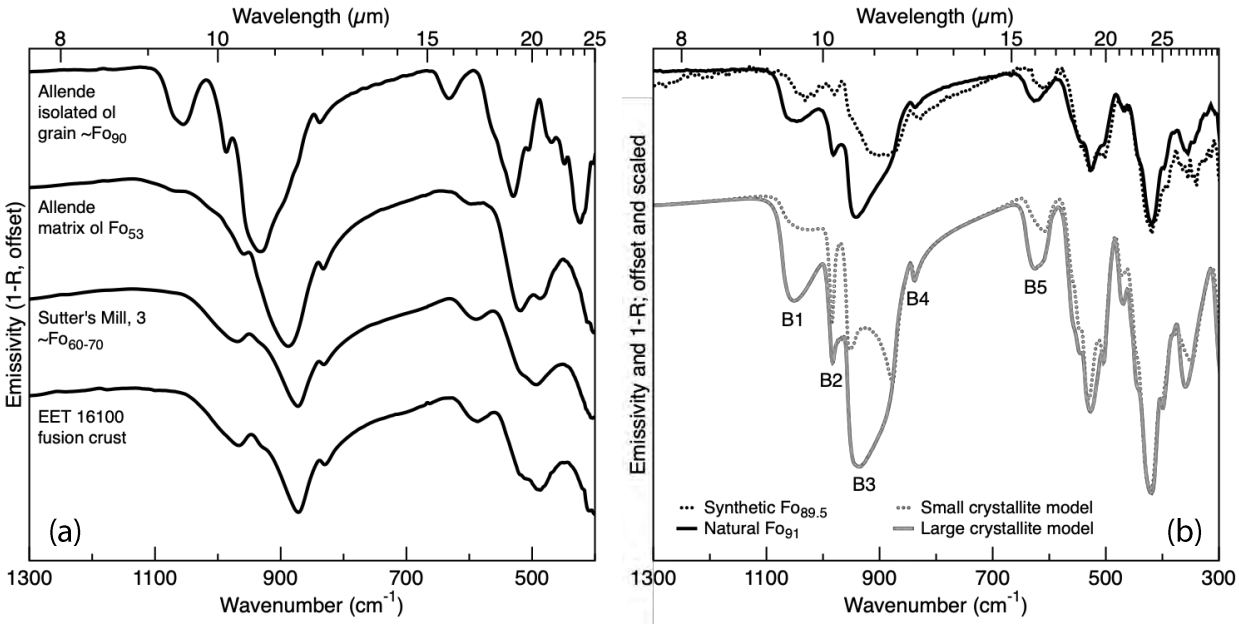

Figure 2.

347

This is the peer-reviewed, final accepted version for American Mineralogist, published by the Mineralogical Society of America.
The published version is subject to change. Cite as Authors (Year) Title. American Mineralogist, in press.
DOI: https://doi.org/10.2138/am-2020-7602. http://www.minsocam.org/

Revision 1

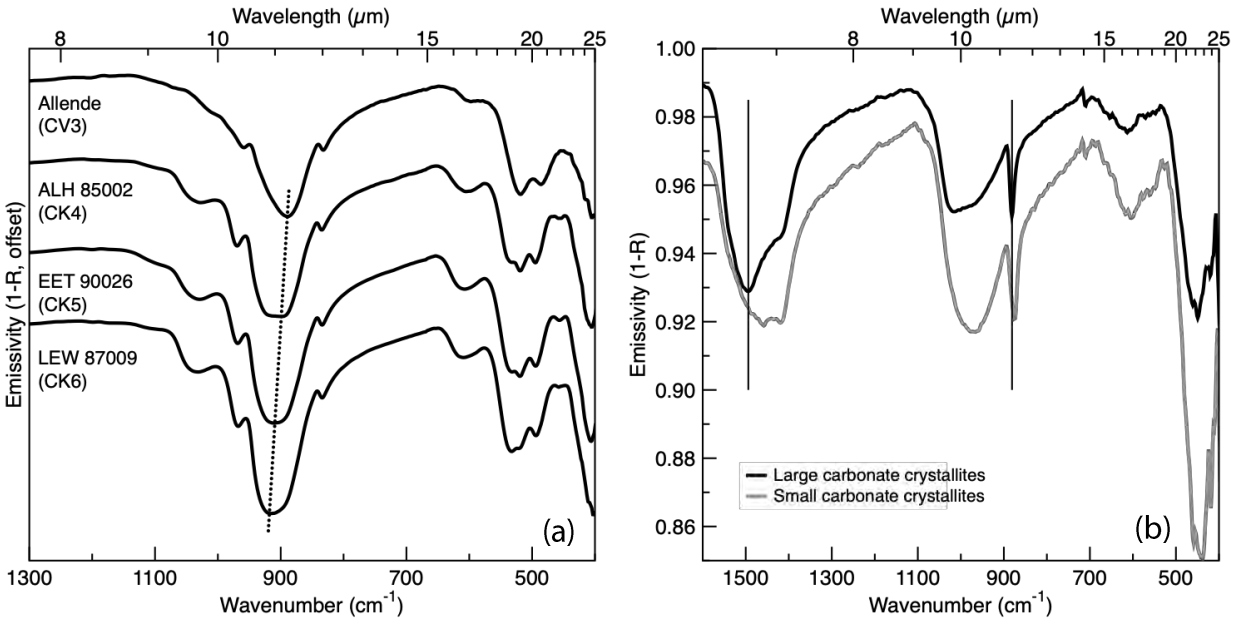

Figure 3.

348